

Magnetized Accretion Disks with Outflows for Changing-look AGNs

WEN-BIAO WU¹ AND WEI-MIN GU¹

¹*Department of Astronomy, Xiamen University, Xiamen, Fujian 361005, P. R. China; guwm@xmu.edu.cn*

ABSTRACT

Changing-look active galactic nuclei (CL-AGNs) challenges the standard accretion theory owing to its rapid variability. Recent numerical simulations have shown that, for the sub-Eddington accretion case, the disk is magnetic pressure-dominated, thermally stable, and geometrically thicker than the standard disk. In addition, outflows were found in the simulations. Observationally, high blueshifted velocities absorption lines indicate that outflows exist in AGNs. In this work, based on the simulation results, we investigate the magnetic pressure-dominated disk, and find that the accretion timescale is significantly shorter than that of the standard thin disk. However, such a timescale is still longer than that of the CL-AGNs. Moreover, if the role of outflows is taken into account, then the accretion timescale can be even shortened. By the detailed comparison of the theoretical accretion timescale with the observations, we propose that the magnetic pressure-dominated disk incorporating outflows can be responsible for the rapid variability of CL-AGNs.

Keywords: Accretion (14) — Active galactic nuclei (16) — Galaxy accretion disks (562) — Magnetic fields (994)

1. INTRODUCTION

Active galactic nuclei (AGNs) have strong flux variations from infrared to X-rays and are typically classified into two types: type 1, which shows broad emission lines, and type 2, which does not. According to the AGNs unified model, these two types differ in their orientations with respect to the observer's line of sight to the dust torus surrounding the AGNs (e.g., Antonucci 1993). However, an increasing number of multi-wavelength observations (including X-ray (e.g., Krumpe et al. 2017; Noda & Done 2018; Parker et al. 2019; Jana et al. 2021), infrared (e.g., Sheng et al. 2017; Yang et al. 2018; Kokubo & Minezaki 2020), and radio (e.g., Koay et al. 2016; Panessa et al. 2019; Yang et al. 2021; Lyu et al. 2021)) have identified a sub-class of AGNs referred to as changing-look AGNs (CL-AGNs), which are capable of transforming from type 1 to type 2 or vice versa over relatively short timescales. Due to the difficulties in explaining the timescale of CL-AGNs using the standard model (Shakura & Sunyaev 1973, hereafter SSD), it has become an increasingly interesting topic.

Several schemes have been proposed to explain the contradictions between theory and observation. The obscuration mechanism, based on the AGNs unified model (Goodrich & Miller 1989) where obstructions enter or leave our line of sight, can cause the appearance or disappearance of broad emission lines. However, this scheme is ruled out due to significant variation of CL-AGNs' mid-infrared emissions and the absence of polarization or weak polarization (e.g., MacLeod et al. 2016; Sheng et al. 2017; Hutsemékers et al. 2019). Another candidate is tidal disruption events (e.g., Merloni et al. 2015; Runnoe et al. 2016; Ricci et al. 2020), which predicts a change in the light curve with $t^{-5/3}$. Although it explains some cases, most observations do not support this model (Sheng et al. 2020). It is generally accepted that these intrinsic changes from the accretion disk and variations in the accretion rate dominate this phenomenon. However, the viscosity timescale of the standard disk, which varies with the accretion rate, is much larger than that of the CL-AGNs (e.g., Stern et al. 2018; Ricci & Trakhtenbrot 2022). Therefore, new models or modifications to the standard model have been proposed to address the issue. The role of the magnetic field in accretion disks has been studied and applied to the CL-AGNs (e.g., Dexter & Begelman 2019; Feng et al. 2021; Scepi et al. 2021, 2023). The limit cycle of magnetically dominated disks or disk instabilities located in the narrow region between the inner ADAF and the outer standard disk is used to explain the repeating CL-AGNs (e.g., Sniegowska et

al. 2020; Pan et al. 2021; Kaur et al. 2022). Wang & Bon (2020) demonstrated that tidal interaction between disks in supermassive black hole binaries can also trigger CL-AGNs.

The standard thin disk model has served as the foundation for understanding various astronomical phenomena since its proposal. However, it still faces challenges such as observations of cataclysmic variables and low-mass X-rays binaries, where the disk appears to be geometrically thicker than expected (see Begelman & Pringle (2007) for details). Most recently, numerical simulations (Huang et al. 2023) have shown that, for the sub-Eddington accretion case, the disk is dominated by the magnetic pressure and exhibits distinct properties from the standard thin disk. The magnetic pressure-dominated accretion disk is thermally stable, geometrically thicker than the standard thin disk, and has flatter effective temperature profiles. In addition, outflows were found in the simulations. These features are consistent with Begelman & Pringle (2007)'s magnetically dominated viscous disks and some previous numerical simulations (e.g., Salvesen et al. 2016; Sadowski 2016; Jiang et al. 2019) except for outflow. The two-dimensional radiation-magnetohydrodynamic numerical simulation by Ohsuga & Mineshige (2011) likewise discovers outflows driven by magnetic pressure on standard-type thin disks.

Highly blueshifted absorption lines are frequently detected in the UV and X-ray spectra of AGNs (e.g., Tombesi et al. 2010; Serafinelli et al. 2019), indicating the presence of high-velocity winds/outflows in these systems. These outflows, particularly ultrafast ones, are presumed to originate in the inner regions of accretion disks and could be powered by the magnetic field (e.g., Yang et al. 2021; Wang et al. 2022). Recent observations have also validated the existence of outflows in CL-AGNs, such as MrK590 (Gupta et al. 2015) and NGC1566 (Jana et al. 2021). In this study, we utilized the results of numerical simulations to elucidate the CL-AGNs phenomenon by considering the impact of outflows. The remainder is organized as follows. In Section 2, we provide basic physics and equations for our model. Section 3 shows numerical results and analyses. Section 4 presents the conclusions and discussion.

2. BASIC EQUATIONS

For simplicity, a steady-state axisymmetric magnetized accretion disk with outflows is considered under the well-known pseudo-Newtonian potential $\Phi = -GM_{\text{BH}}/(R - R_{\text{g}})$ (Paczynski & Wiita 1980), where M_{BH} is the mass of the black hole and $R_{\text{g}} = 2GM_{\text{BH}}/c^2$ is the Schwarzschild radius. Therefore, we assume the angular velocity is Keplerian, i.e., $\Omega = \Omega_{\text{K}} = [GM_{\text{BH}}/R(R - R_{\text{g}})]^{1/2}$.

In this work, the magnetic pressure $P_{\text{m}} = B^2/8\pi$, B is the mean mid-plane magnetic field strength. The gas pressure $P_{\text{g}} = \rho k_{\text{B}} T_{\text{c}}/\mu m_{\text{p}}$, the radiation pressure $P_{\text{r}} = aT_{\text{c}}^4/3$, where T_{c} is the mid-plane temperature, ρ is the mid-plane density, $\mu = 0.617$ is the mean molecular weight, k_{B} is the Boltzmann constant, and a is the radiation constant. We adopt Begelman & Pringle (2007) in assuming that the magneto-rotational instability-riven dynamo could amplify the turbulent (toroidal) field until saturation. The saturation is determined by the Alfvén speed $V_{\text{A}} \equiv \sqrt{P_{\text{m}}/\rho}$ and roughly equals the geometric means of the Keplerian velocity V_{K} and the gas sound speed $c_{\text{g}} = \sqrt{P_{\text{g}}/\rho}$, i.e.,

$$V_{\text{A}}^2 = \lambda V_{\text{K}} c_{\text{g}} , \quad (1)$$

where we have introduced a parameter λ , which represents the strength of the turbulent (toroidal) magnetic field, and λ is in the range $[0, 1]$. The condition $\lambda = 1$ corresponds to the saturation case of the turbulent (toroidal) magnetic field and has been observed by numerical simulations (e.g., Huang et al. 2023).

Due to the additional magnetic pressure, the total pressure $P = P_{\text{m}} + P_{\text{g}} + P_{\text{r}}$, the sound speed is written as

$$c_{\text{s}}^2 = \frac{P}{\rho} . \quad (2)$$

Numerical simulations have demonstrated the above magnetically dominated viscous disks (e.g., Salvesen et al. 2016; Sadowski 2016; Jiang et al. 2019; Huang et al. 2023). The model shows a geometrically thicker disk and higher color temperatures, which would be stable against thermal and viscous instabilities. In addition, outflows were found in the simulations (Huang et al. 2023). The two-dimensional radiation-magnetohydrodynamic numerical simulation of Ohsuga & Mineshige (2011) also found outflows driven by magnetic pressure on standard-type thin disks (in their numerical simulation, the toroidal component of the magnetic field is dominant, i.e., $|B_{\varphi}|/B_{\text{p}} > 1$). Taking inspiration from the simulations above, we developed a new outflow model. The fundamental equations describing accretion disks with outflows employed in this study can be found in our previous work (Wu et al. 2022). The continuity equation is

$$\dot{M} = -2\pi R \Sigma V_{\text{R}} , \quad (3)$$

where V_R is the inflow speed, which is defined to be negative when the flow is inward, and Σ is the surface density

$$\Sigma = 2\rho H . \quad (4)$$

The scaleheight can be redefined based on the above analysis

$$H = \frac{c_s}{\Omega_K} , \quad (5)$$

Similarly, we redefine the kinematic viscosity as

$$\nu = \alpha c_s H , \quad (6)$$

where α is the viscosity parameter. In principle, α is related to the magnetization of the disk (Salvesen et al. 2016). Thus, for high viscosity, such as $\alpha = 0.1$, the parameter λ may not be negligible. The relationship between α and the magnetization of the disk is beyond the scope of this paper. For simplicity, we take both α and λ as free parameters in this work.

Due to the effect of outflow, we assume that the mass accretion rate varies with the radius (Ferreira & Pelletier 1995; Blandford & Begelman 1999) $\dot{M} = \dot{M}_{\text{out}}(R/R_{\text{out}})^p$, where \dot{M}_{out} is the mass accretion rate at the outer boundary R_{out} , in the present investigation, we set p as a free parameter.

The azimuthal momentum equation is reduced to the algebraic form (Wu et al. 2022):

$$\nu\Sigma = \frac{\dot{M}fg^{-1}}{3\pi} \left(1 - \frac{l^2p}{p + \frac{1}{2}} \right) , \quad (7)$$

where $g = -(2/3)(d \ln \Omega_K / d \ln R)$ and the factor $f = 1 - [\Omega_K(3R_g)/\Omega_K(R)](3R_g/R)^{p+2}$. l is the parameter that characterizes the angular momentum taken away by the outflow (Knigge 1999). In this study, we set $l > 1$ due to the presence of a strong magnetic field.

The energy equation is written as

$$Q_{\text{vis}} = Q_{\text{rad}} , \quad (8)$$

where Q_{vis} and Q_{rad} are the viscous heating rate and the radiative cooling rate, respectively. Their expressions are as follows (Wu et al. 2022),

$$Q_{\text{vis}} = \frac{3\dot{M}\Omega_K^2 fg}{4\pi} \left(1 - \frac{l^2p}{p + \frac{1}{2}} \right) , \quad (9)$$

$$Q_{\text{rad}} = \frac{16\sigma T_c^4}{3\tau} , \quad (10)$$

where $\tau = \kappa_{\text{es}}\rho H$ represents the optical depth, with $\kappa_{\text{es}} = 0.34 \text{ cm}^2 \text{ g}^{-1}$ being the electric scattering opacity. In the inner region of the accretion disk, electric scattering opacity dominates over free-free absorption, leading the latter to be neglected when calculating the disk's structure.

The equation of state concerning the sound speed c_s is

$$\rho c_s^2 = \rho V_A^2 + \frac{\rho k_B T_c}{\mu m_p} + \frac{1}{3} a T_c^4 . \quad (11)$$

Considering the viscosity prescription, we have

$$\frac{3}{2} \rho \nu \Omega_K = \alpha P . \quad (12)$$

By solving the ten equations, Equations (1-8), and (11-12), for the ten variables V_A , P , c_g , c_s , H , Σ , V_R , ν , ρ and T_c with given parameters M_{BH} , α , \dot{M} , λ , and l . We obtain the accretion timescale $t_{\text{acc}} = -R/V_R$. In the following calculations, we define as $\dot{M}_{\text{Edd}} = 16L_{\text{Edd}}/c^2 = 64\pi GM_{\text{BH}}/\kappa_{\text{es}}c$, and fix $R_{\text{out}} = 50R_g$, where a typical region of the optical/UV emission.

3. NUMERICAL RESULTS

Before detailed numerical calculations, we do some analysis of the basic characteristic timescales of the accretion disk, including the dynamical, thermal, and viscous timescales. Their expressions are as follows (Frank et al. 1985; Kato et al. 2008),

$$t_{\text{dyn}} \sim \frac{1}{\Omega_{\text{K}}}, \quad (13)$$

$$t_{\text{th}} \sim \frac{1}{\alpha \Omega_{\text{K}}}, \quad (14)$$

$$t_{\text{vis}} \sim \frac{1}{\alpha \Omega_{\text{K}}} \left(\frac{H_{\text{SSD}}}{R} \right)^{-2}, \quad (15)$$

Regarding the observed timescales of CL-AGNs, t_{dyn} and t_{th} are too short, while t_{vis} is too long (e.g., Stern et al. 2018; Ricci & Trakhtenbrot 2022). From Equations (14) and (15), it is seen that $t_{\text{th}} \propto (H_{\text{SSD}}/R)^0$ and $t_{\text{vis}} \propto (H_{\text{SSD}}/R)^{-2}$. Some researchers (e.g., Stern et al. 2018; Ricci & Trakhtenbrot 2022) have suggested that setting $t \propto (H_{\text{SSD}}/R)^{-1}$ may help address these inconsistencies. When outflows are not considered (i.e., $l = 0, p = 0$), this corresponds to the case of magnetically dominated viscous disks. By using Equations (3) and (6), Equation (7) can reduce to

$$V_{\text{R}} = -\frac{3\nu f^{-1}g}{2R}, \quad (16)$$

then, the accretion timescale

$$t_{\text{acc}} = -\frac{R}{V_{\text{R}}} = \frac{2fg^{-1}}{3\alpha\Omega_{\text{K}}} \left(\frac{H}{R} \right)^{-2} \propto \left(\frac{H}{R} \right)^{-2}. \quad (17)$$

For $\lambda = 1$, $V_{\text{A}} \gg c_{\text{g}}$, using Equations (1-2) and (5), we have $c_{\text{s}} \approx V_{\text{A}}$, then

$$t_{\text{acc}} \propto \left(\frac{H}{R} \right)^{-2} \propto \left(\frac{c_{\text{g}}}{V_{\text{K}}} \right)^{-1} \propto \left(\frac{H_{\text{SSD}}}{R} \right)^{-1}. \quad (18)$$

According to the above analysis, we have shown that $t_{\text{acc}} \propto (H/R)^{-2} \sim (H_{\text{SSD}}/R)^{-1}$. However, based on the following numerical calculations, we find that $t_{\text{acc}} \propto (H_{\text{SSD}}/R)^{-1}$ cannot fully explain the rapid variability of CL-AGNs. On the other hand, we propose that outflows play an important role in explaining the phenomenon of CL-AGNs.

Figure 1 shows the relationship of outflow parameter p and the strength of the turbulent (toroidal) magnetic field λ for a given timescale when the $L_{\text{bol}}/L_{\text{Edd}} = 0.05$, where $M_{\text{BH}} = 10^8 M_{\odot}$, $\alpha = 0.1$, and $L_{\text{bol}} (= \int 2\pi R Q_{\text{rad}} dR)$ is the bolometric luminosity. The dashed line represents ($l = \sqrt{2}$) and the solid line corresponds to ($l = 2$). We would like to stress that, the scaleheight of the disk in our model (magnetically dominated viscous disks with outflows), is significantly larger than that of a standard thin disk (see Appendix A for the derivation of scaleheight). Therefore, it is possible to further shorten the accretion timescale. The blue, red, and black lines represent 20, 10, and 5 years, respectively. For comparison, we calculated the accretion timescale of the standard thin disks ($\lambda = 0$, $l = 0$, $p = 0$), note that for standard thin disks: $\lambda \ll 1$. In this work, for simplicity, we followed the conventional approach $\lambda = 0$ for standard thin disks, as described in some classic literature, e.g., Eq.(5.36) of Frank et al. (2002) and Eq. (3.41) of Kato et al. (2008)) and the magnetically dominated viscous disks ($0 < \lambda \leq 1$, $l = 0$, $p = 0$) under the same conditions ($\alpha = 0.1$, $L_{\text{bol}}/L_{\text{Edd}} = 0.05$): $t_{\text{acc}} \sim 3.35 \times 10^3$ year and $t_{\text{acc}} \geq 63.36$ year. Our calculations demonstrate that if the role of outflows is considered in the magnetic pressure-dominated disk, the accretion timescale can be shortened to several decades or a few years.

To further understand the impact of the outflow, we adopt $M_{\text{BH}} = 10^8 M_{\odot}$ and fix $\lambda = 1$ based on simulation results (Huang et al. 2023). We set $l = 2$, which corresponds to the case that significant angular momentum is carried away by outflows. The range of the parameter p is constrained by the given values of λ and l . In our case, the range $0 < p \leq 0.16$ corresponds to $\lambda = 1$ and $l = 2$. In addition, by varying the viscosity parameter α ($0.01 \sim 0.3$) and the range of L_{bol} ($0.001 \leq L_{\text{bol}}/L_{\text{Edd}} \leq 0.1$), we therefore obtain a decade range in accretion timescale in Figure 2. The blue region is the accretion timescale of standard thin disks, the green region is the accretion timescale of magnetically dominated viscous disks, and the yellow region takes into account the role of outflows. Black dots denote the high state

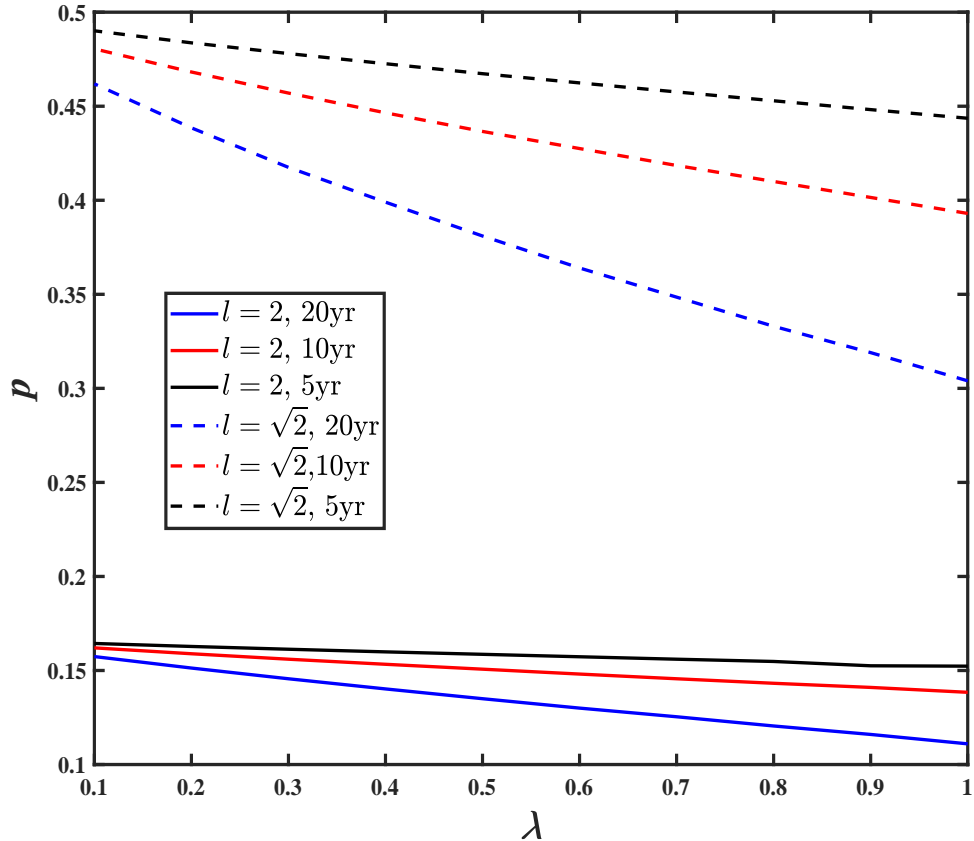


Figure 1. Timescales are shown in the $\{p, \lambda\}$ - plane for a given $L_{\text{bol}}/L_{\text{Edd}} = 0.05$. The dashed line represents ($l = \sqrt{2}$) and the solid line corresponds to ($l = 2$). Each of the color lines corresponds to a specific value on the timescale.

(turn-on) of CL-AGNs discovered by Jin et al. (2022) via SDSS, with physical quantities listed in Table 1. Figure 2 shows that the timescale of magnetically dominated viscous disks is significantly shorter than that of standard thin disks, but still longer than the observed timescale. However, when the angular momentum is carried away by the outflow, the radial velocity of the accretion disk can be significantly increased, as shown in Equation (A2). Thus, magnetically dominated viscous disks with outflows can further shorten the accretion timescale and satisfy the rapid variability observed in CL-AGNs, as shown by the yellow region in Figure 2.

Based on the preceding analysis, our model predicts a timescale that can be as short as several years, which aligns with the observed timescale of CL-AGNs. However, this result is based on a fixed mass assumption and may not accurately reflect timescales for CL-AGNs with different masses. Figure 3 illustrates the variations in accretion time with mass. Similar to Figure 2, we choose $\lambda = 1$, $l = 2$, and $0 < p \leq 0.16$. By varying α ($0.01 \sim 0.3$) and L_{bol} ($0.001 \leq L_{\text{bol}}/L_{\text{Edd}} \leq 0.1$), as well as a given range for M_{BH} ($10^6 M_{\odot} \leq M_{\text{BH}} \leq 10^9 M_{\odot}$), we therefore obtain a decade range in accretion timescale. As depicted in Figure 3, while the magnetically dominated viscous disks model can satisfy CL-AGNs with masses less than $10^{7.5} M_{\odot}$, it is ineffective for higher masses. In contrast, our model can accommodate all sources' timescales. Therefore, the magnetic pressure-dominated disk model, with outflows taken into account, appears to be particularly promising for resolving the inconsistencies between observed timescales and disk theory.

4. CONCLUSIONS AND DISCUSSION

In this work, following the recent simulation results of Huang et al. (2023), we have investigated the accretion timescale of the magnetic pressure-dominated accretion disk. Our results show that, even the timescale is significantly

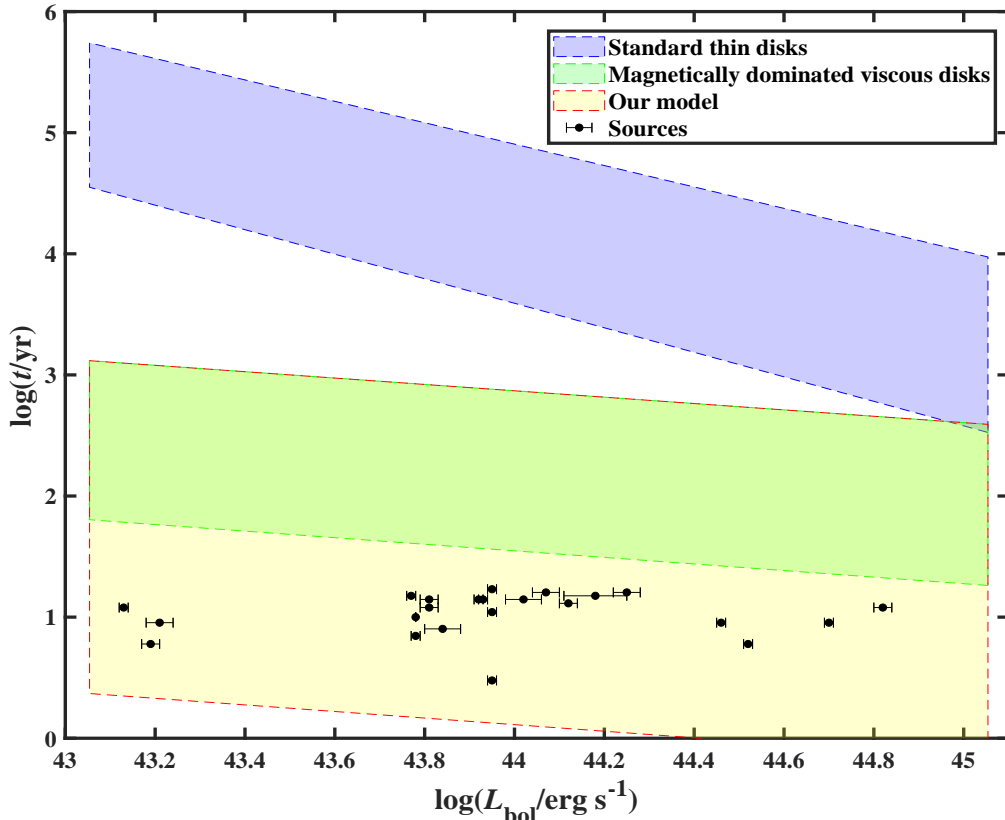


Figure 2. The accretion timescale of accretion disks at $M_{\text{BH}} = 10^8 M_{\odot}$ for different α and L_{bol} . The regions of color correspond to the cases for the standard thin disks (blue), magnetically dominated viscous disks (green), and our model (magnetically dominated viscous disks with outflows, yellow). The black dots are the high state (turn-on) of CL-AGNs in Table 1.

shorter than that of the standard thin disk, it is still beyond the rapid variability of CL-AGNs. Furthermore, by taking into account the role of outflows, which were generally found in simulations and observations, we have shown that the accretion timescale can be even shortened. By the detailed comparison of the theoretical accretion timescale with the observations, we propose that the magnetic pressure-dominated disk with outflows can be responsible for the rapid variability of CL-AGNs.

The effects of magnetic fields on accretion disks have been extensively studied, and some early research (Ferreira & Pelletier 1995; Ferreira 1997; Jacquemin-Ide et al. 2019) found that magnetic winds can significantly decrease the accretion timescale. This finding has been confirmed by numerical simulations (Jacquemin-Ide et al. 2021; Scepi et al. 2023) and has been used to explain observed phenomena such as YSOs (Combet & Ferreira 2008; Martel & Lesur 2022) and X-ray binaries (Ferreira et al. 2006; Marcel et al. 2018). Full MHD models (Ferreira 1997) relate various parameters, such as p with disk magnetization, α with disk magnetization, and l with p . However, these models do not fully consider the role of magnetic (turbulence) pressure. We would point out that our model includes magnetic pressure and utilizes a simple parameterization, and it is worth further investigation on the relationship among these parameters.

Quasi-periodic eruptions (QPEs) are a newly discovered type of changing-look phenomenon characterized by rapid and extreme X-ray bursts with mass $M_{\text{BH}} \sim 10^5\text{--}6 M_{\odot}$, and periods as short as a few hours (e.g., Miniutti et al. 2019; Giustini et al. 2020; Chakraborty et al. 2021; Arcodia et al. 2021). However, these short timescales cannot be explained even at $R = 50R_g$ and $\alpha = 0.3$ using our present one-zone model. In order to interpret QPEs, a thicker disk may be necessary. Begelman et al. (2015) proposed a vertically stratified model with a larger characteristic scale height $H \sim R$ which agrees with Bai & Stone (2013)’s vertically stratified, local shearing box ideal MHD. Subsequent numerical simulations (Salvesen et al. 2016) have also confirmed this model. In addition, Bai & Stone (2013) also

Table 1. Information about sources.

Name	L_{bol}		$M_{\text{BH,vir}}$	Δt (yr)
	$\log(\text{erg s}^{-1})$		$\log(M/M_{\odot})$	yr
	on	off		
(1)	(2)		(3)	(4)
J0126-0839	44.52 ± 0.01	43.72 ± 0.03	$7.70^{+0.11}_{-0.10}$	6.0
J0159+0033	44.70 ± 0.01	44.18 ± 0.01	$7.71^{+0.12}_{-0.10}$	9.0
ZTF18aaabltn	43.13 ± 0.01	42.25 ± 0.11	$7.13^{+0.13}_{-0.11}$	12.0
J0831+3646	43.81 ± 0.02	43.35 ± 0.05	$8.05^{+0.18}_{-0.17}$	14.0
J0909+4747	43.92 ± 0.01	43.50 ± 0.01	$7.32^{+0.13}_{-0.12}$	14.0
J0937+2602	43.84 ± 0.04	43.72 ± 0.01	$7.33^{+0.20}_{-0.19}$	8.0
J1003+3525	43.81 ± 0.03	43.50 ± 0.02	$8.15^{+0.16}_{-0.15}$	12.0
J1104+6343	43.19 ± 0.02	43.07 ± 0.06	$7.72^{+0.12}_{-0.10}$	6.0
J1110-0003	44.25 ± 0.03	44.07 ± 0.01	$8.02^{+0.12}_{-0.11}$	16.0
J1115+0544	43.93 ± 0.01	42.70 ± 0.07	$7.25^{+0.10}_{-0.08}$	14.0
J1132+0357	44.12 ± 0.02	42.86 ± 0.04	$7.17^{+0.14}_{-0.13}$	13.0
ZTF18aasuray	43.95 ± 0.01	42.54 ± 0.02	$7.24^{+0.16}_{-0.15}$	17.0
ZTF18aasszwr	45.20 ± 0.00	43.01 ± 0.06	$8.68^{+0.10}_{-0.09}$	16.0
ZTF18aahiqf	43.77 ± 0.01	42.70 ± 0.04	$8.26^{+0.15}_{-0.13}$	15.0
J1259+5515	44.02 ± 0.04	43.48 ± 0.06	$7.39^{+0.11}_{-0.10}$	14.0
J1319+6753	44.07 ± 0.03	43.81 ± 0.02	$7.17^{+0.18}_{-0.17}$	16.0
J1358+4934	43.95 ± 0.01	43.35 ± 0.02	$7.15^{+0.13}_{-0.12}$	3.0
J1447+2833	44.46 ± 0.01	44.03 ± 0.00	$7.46^{+0.12}_{-0.10}$	9.0
ZTF18aajupnt	42.04 ± 0.13	41.92 ± 0.15	$6.45^{+0.11}_{-0.10}$	16.0
J1533+0110	43.78 ± 0.01	43.49 ± 0.02	$7.38^{+0.11}_{-0.10}$	7.0
J1545+2511	43.95 ± 0.01	43.70 ± 0.01	$7.34^{+0.11}_{-0.10}$	11.0
J1550+4139	44.18 ± 0.07	43.53 ± 0.05	$7.25^{+0.10}_{-0.08}$	15.0
J1552+2737	43.21 ± 0.03	42.84 ± 0.05	$7.94^{+0.12}_{-0.11}$	9.0
J1554+3629	44.82 ± 0.02	42.93 ± 0.08	$8.00^{+0.15}_{-0.14}$	12.0
PS1-13cbe	43.78 ± 0.00	42.54 ± 0.09	$6.89^{+0.10}_{-0.08}$	10.0

NOTE—Column 2: The bolometric luminosity of CL-AGNs “turn-on” and “turn-off” (high and low states). Column 3: the virial black hole mass of CL-AGNs. Column 4: The lag between the “turn-on” and “turn-off” epochs in CL-AGNs. More physical quantities and derivation processes can be found in [Jin et al. \(2022\)](#).

shows that a magnetocentrifugal mechanism could excite a strong outflow. Therefore, our future work will focus on a new outflow model based on these findings to explain the QPE phenomenon.

We thank Zhi-Xiang Zhang for helpful discussions, and the anonymous referee for constructive suggestions that improved the paper. This work was supported by the National Natural Science Foundation of China under grants 11925301, 12033006, and 12221003.

APPENDIX

A. EXPRESSION OF SCALEHEIGHT

In this Appendix, we will derive the detailed expression of scaleheight, which is mentioned in Section 3.

For $\lambda = 1$, $V_A \gg c_g$, according to Equations (1-2) and (5), the scaleheight takes the form:

$$\frac{H}{R} = \left(\frac{c_g}{V_K} \right)^{1/2}. \quad (\text{A1})$$

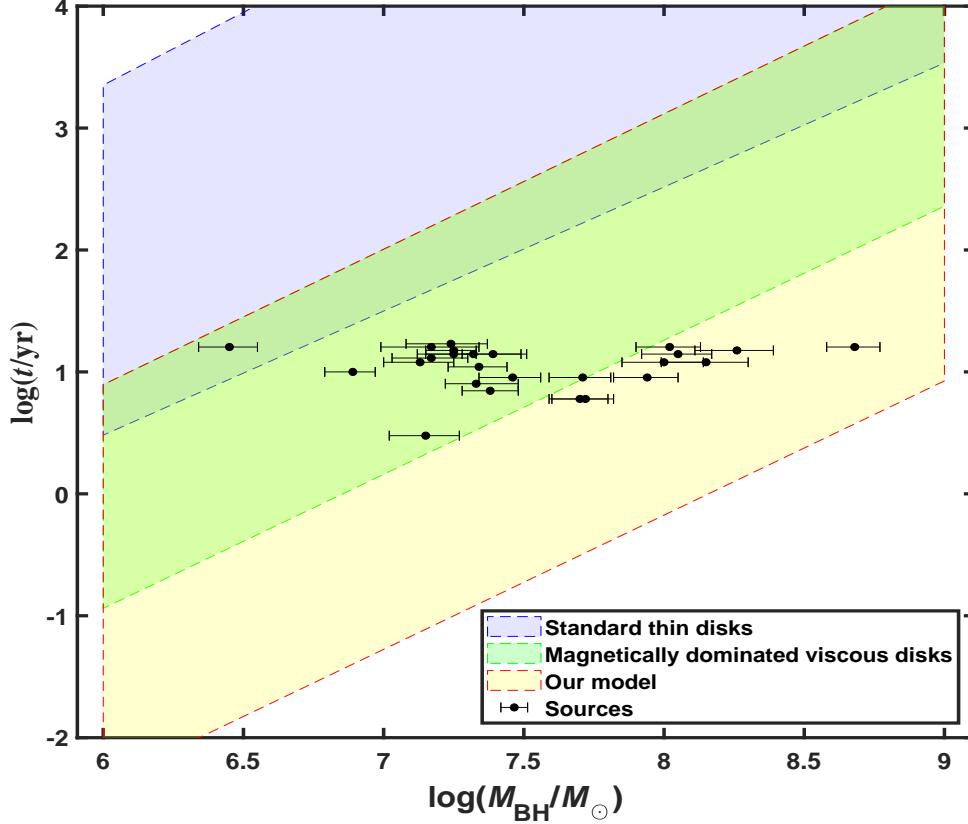


Figure 3. The variations of the accretion timescale with mass under the $\lambda = 1, l = 2, \alpha = 0.01 \sim 0.3, L_{\text{bol}}/L_{\text{Edd}} = 0.001 \sim 0.1$. The meaning of the colors and symbols is the same as in Figure 2. For the standard thin disks, the accretion timescale is much larger than the observed timescale. Magnetically dominated viscous disks only explain part of the CL-AGNs. However, our model (magnetically dominated viscous disks with outflows) can naturally explain all the observed sources.

Combining Equations (3) and (6-7), we have

$$V_R = -\frac{3}{2} \frac{\alpha f^{-1} g}{R} \left(1 - \frac{l^2 p}{p + 1/2}\right)^{-1} c_g. \quad (\text{A2})$$

The surface density is

$$\Sigma = \frac{\dot{M} f g^{-1}}{3\pi \alpha c_g R} \left(1 - \frac{l^2 p}{p + 1/2}\right). \quad (\text{A3})$$

Defining $\dot{m} \equiv \dot{M}/\dot{M}_{\text{Edd}}$ and $x \equiv R/R_g$, we obtain an expression for the optical depth through the disk:

$$\tau = \frac{16}{3} \frac{\dot{m} f g^{-1} c}{\alpha c_g} x^{-1} \left(1 - \frac{l^2 p}{p + 1/2}\right). \quad (\text{A4})$$

Q_{vis} can be reduced to

$$Q_{\text{vis}} = \frac{6\dot{m} c^5 f g}{\kappa_{\text{es}} G M_{\text{BH}}} x^{-1} (x-1)^{-2} \left(1 - \frac{l^2 p}{p + 1/2}\right), \quad (\text{A5})$$

Due to $Q_{\text{rad}} = 4P_r c/\tau = Q_{\text{vis}}$, we can get

$$P_r = \frac{8\dot{m}^2 c^5 f^2}{\alpha \kappa_{\text{es}} G M_{\text{BH}}} x^{-2} (x-1)^{-2} \left(1 - \frac{l^2 p}{p + 1/2}\right)^2 c_g^{-1}. \quad (\text{A6})$$

According to the radiation pressure, we have

$$T_c = \left(\frac{3P_r}{a} \right)^{1/4}. \quad (\text{A7})$$

For $P_g \gg P_r$, we have

$$c_g = \left(\frac{k_B T_c}{\mu m_p} \right)^{1/2}. \quad (\text{A8})$$

Using Equations (A6-A8), we get the expression of c_g :

$$c_g = \left(\frac{k_B}{\mu} m_p \right)^{4/9} \left[\frac{24\dot{m}^2 c^5 f^2}{a\alpha\kappa_{\text{es}} GM_{\text{BH}}} x^{-2} (x-1)^{-2} \left(1 - \frac{l^2 p}{p+1/2} \right)^2 \right]^{1/9}. \quad (\text{A9})$$

Substituting Equation (A9) into (A1) to get the H/R :

$$\frac{H}{R} = 3.5 \times 10^{-2} (\alpha m)^{-1/18} \dot{m}^{1/9} x^{-13/36} (x-1)^{7/18} \left(1 - \frac{l^2 p}{p+1/2} \right)^{1/9} f^{1/9}, \quad (\text{A10})$$

where $m = M_{\text{BH}}/(10^8 M_\odot)$. This is similar to the case of Scepi et al. (2023) with $H/R = 0.03$.

For non-outflow cases ($l = 0, p = 0$, see Equation (19) of Begelman & Pringle (2007)), we have

$$\frac{H}{R} = 3.5 \times 10^{-2} (\alpha m)^{-1/18} \dot{m}^{1/9} x^{-13/36} (x-1)^{7/18} f^{1/9}, \quad (\text{A11})$$

For $\lambda = 0, l = 0, p = 0$, our model returns to the standard thin model. Similarly, we can obtain (see, e.g., Equation (3.66) of (Kato et al. 2008))

$$\frac{H_{\text{SSD}}}{R} = 2.4 \times 10^{-3} (\alpha m)^{-1/10} \dot{m}^{1/5} x^{-13/20} (x-1)^{7/10} f^{1/5}. \quad (\text{A12})$$

By comparing Equation (A11) with Equation (A12), we find $H_{\text{SSD}}/R \sim (H/R)^{1.8}$, which is quite close to the simple analytic result $H_{\text{SSD}}/R \sim (H/R)^2$ (Equation (18)).

REFERENCES

- Antonucci, R. 1993, *ARA&A*, 31, 473.
doi:10.1146/annurev.aa.31.090193.002353
- Arcodia, R., Merloni, A., Nandra, K., et al. 2021, *Nature*, 592, 704. doi:10.1038/s41586-021-03394-6
- Blandford, R. D. & Begelman, M. C. 1999, *MNRAS*, 303, L1. doi:10.1046/j.1365-8711.1999.02358.x
- Begelman, M. C. & Pringle, J. E. 2007, *MNRAS*, 375, 1070. doi:10.1111/j.1365-2966.2006.11372.x
- Begelman, M. C., Armitage, P. J., & Reynolds, C. S. 2015, *ApJ*, 809, 118. doi:10.1088/0004-637X/809/2/118
- Bai, X.-N. & Stone, J. M. 2013, *ApJ*, 767, 30. doi:10.1088/0004-637X/767/1/30
- Chakraborty, J., Kara, E., Masterson, M., et al. 2021, *ApJL*, 921, L40. doi:10.3847/2041-8213/ac313b
- Combet, C. & Ferreira, J. 2008, *Astronomy and Astrophysics*, 479, 481. doi:10.1051/0004-6361:20078734
- Dexter, J. & Begelman, M. C. 2019, *MNRAS*, 483, L17. doi:10.1093/mnrasl/sly213
- Frank, J., King, A. R., & Raine, D. J. 1985, *Cambridge Astrophysics Series*, Cambridge: University Press, 1985
- Frank, J., King, A., & Raine, D. J. 2002, *Accretion Power in Astrophysics*, by Juhan Frank and Andrew King and Derek Raine, pp. 398. ISBN 0521620538. Cambridge, UK: Cambridge University Press, February 2002., 398
- Ferreira, J. & Pelletier, G. 1995, *Astronomy and Astrophysics*, 295, 807
- Ferreira, J. 1997, *Astronomy and Astrophysics*, 319, 340. doi:10.48550/arXiv.astro-ph/9607057
- Ferreira, J., Petrucci, P.-O., Henri, G., et al. 2006, *Astronomy and Astrophysics*, 447, 813. doi:10.1051/0004-6361:20052689
- Feng, J., Cao, X., Li, J.-. wen ., et al. 2021, *ApJ*, 916, 61. doi:10.3847/1538-4357/ac07a6

- Goodrich, R. W. & Miller, J. S. 1989, *ApJL*, 346, L21.
doi:10.1086/185569
- Gupta, A., Mathur, S., & Krongold, Y. 2015, *ApJ*, 798, 4.
doi:10.1088/0004-637X/798/1/4
- Giustini, M., Miniutti, G., & Saxton, R. D. 2020, *A&A*, 636, L2. doi:10.1051/0004-6361/202037610
- Hutsemékers, D., Agís González, B., Marin, F., et al. 2019, *A&A*, 625, A54. doi:10.1051/0004-6361/201834633
- Huang, J., Jiang, Y.-F., Feng, H., et al. 2023, *The Astrophysical Journal*, 945, 57.
doi:10.3847/1538-4357/acb6fc
- Jacquemin-Ide, J., Ferreira, J., & Lesur, G. 2019, *Monthly Notices of the Royal Astronomical Society*, 490, 3112.
doi:10.1093/mnras/stz2749
- Jacquemin-Ide, J., Lesur, G., & Ferreira, J. 2021, *Astronomy and Astrophysics*, 647, A192.
doi:10.1051/0004-6361/202039322
- Jiang, Y.-F., Blaes, O., Stone, J. M., et al. 2019, *ApJ*, 885, 144. doi:10.3847/1538-4357/ab4a00
- Jana, A., Kumari, N., Nandi, P., et al. 2021, *MNRAS*, 507, 687. doi:10.1093/mnras/stab2155
- Jana, A., Kumari, N., Nandi, P., et al. 2021, *MNRAS*, 507, 687. doi:10.1093/mnras/stab2155
- Jin, J.-J., Wu, X.-B., & Feng, X.-T. 2022, *ApJ*, 926, 184.
doi:10.3847/1538-4357/ac410c
- Knigge, C. 1999, *MNRAS*, 309, 409.
doi:10.1046/j.1365-8711.1999.02839.x
- Kato, S., Fukue, J., & Mineshige, S. 2008, *Black-Hole Accretion Disks — Towards a New Paradigm* (Kyoto: Kyoto Univ.Press)
- Krumpe, M., Husemann, B., Tremblay, G. R., et al. 2017, *A&A*, 607, L9. doi:10.1051/0004-6361/201731967
- Kokubo, M. & Minezaki, T. 2020, *MNRAS*, 491, 4615.
doi:10.1093/mnras/stz3397
- Koay, J. Y., Vestergaard, M., Bignall, H. E., et al. 2016, *MNRAS*, 460, 304. doi:10.1093/mnras/stw975
- Kaur, K., Stone, N. C., & Gilbaum, S. 2022, *arXiv:2211.00704*
- Lyu, B., Yan, Z., Yu, W., et al. 2021, *MNRAS*, 506, 4188.
doi:10.1093/mnras/stab1581
- MacLeod, C. L., Ross, N. P., Lawrence, A., et al. 2016, *MNRAS*, 457, 389. doi:10.1093/mnras/stv2997
- Merloni, A., Dwelly, T., Salvato, M., et al. 2015, *MNRAS*, 452, 69. doi:10.1093/mnras/stv1095
- Miniutti, G., Saxton, R. D., Giustini, M., et al. 2019, *Nature*, 573, 381. doi:10.1038/s41586-019-1556-x
- Marcel, G., Ferreira, J., Petrucci, P.-O., et al. 2018, *Astronomy and Astrophysics*, 615, A57.
doi:10.1051/0004-6361/201732069
- Martel, É. & Lesur, G. 2022, *Astronomy and Astrophysics*, 667, A17. doi:10.1051/0004-6361/202142946
- Noda, H. & Done, C. 2018, *MNRAS*, 480, 3898.
doi:10.1093/mnras/sty2032
- Ohsuga, K. & Mineshige, S. 2011, *The Astrophysical Journal*, 736, 2. doi:10.1088/0004-637X/736/1/2
- Panessa, F., Baldi, R. D., Laor, A., et al. 2019, *Nature Astronomy*, 3, 387. doi:10.1038/s41550-019-0765-4
- Parker, M. L., Schartel, N., Grupe, D., et al. 2019, *MNRAS*, 483, L88. doi:10.1093/mnras/sly224
- Pan, X., Li, S.-L., & Cao, X. 2021, *ApJ*, 910, 97.
doi:10.3847/1538-4357/abe766
- Paczynsky, B. & Wiita, P. J. 1980, *A&A*, 88, 23
- Runnoe, J. C., Cales, S., Ruan, J. J., et al. 2016, *MNRAS*, 455, 1691. doi:10.1093/mnras/stv2385
- Ricci, C., Kara, E., Loewenstein, M., et al. 2020, *ApJL*, 898, L1. doi:10.3847/2041-8213/ab91a1
- Ricci, C. & Trakhtenbrot, B. 2022, *arXiv:2211.05132*
- Stern, D., McKernan, B., Graham, M. J., et al. 2018, *ApJ*, 864, 27. doi:10.3847/1538-4357/aac726
- Shakura, N. I. & Sunyaev, R. A. 1973, *A&A*, 24, 337
- Sheng, Z., Wang, T., Jiang, N., et al. 2017, *ApJL*, 846, L7.
doi:10.3847/2041-8213/aa85de
- Sheng, Z., Wang, T., Jiang, N., et al. 2020, *The Astrophysical Journal*, 889, 46.
doi:10.3847/1538-4357/ab5af9
- Scepi, N., Begelman, M. C., & Dexter, J. 2021, *MNRAS*, 502, L50. doi:10.1093/mnrasl/slab002
- Scepi, N., Begelman, M. C., & Dexter, J. 2023, *arXiv:2302.10226*. doi:10.48550/arXiv.2302.10226
- Sniegowska, M., Czerny, B., Bon, E., et al. 2020, *A&A*, 641, A167. doi:10.1051/0004-6361/202038575
- Salvesen, G., Armitage, P. J., Simon, J. B., et al. 2016, *MNRAS*, 460, 3488. doi:10.1093/mnras/stw1231
- Sadowski, A. 2016, *MNRAS*, 459, 4397.
doi:10.1093/mnras/stw913
- Serafinelli, R., Tombesi, F., Vagnetti, F., et al. 2019, *Astronomy and Astrophysics*, 627, A121.
doi:10.1051/0004-6361/201935275
- Tombesi, F., Cappi, M., Reeves, J. N., et al. 2010, *Astronomy and Astrophysics*, 521, A57.
doi:10.1051/0004-6361/200913440
- Wu, W.-B., Gu, W.-M., & Sun, M. 2022, *ApJ*, 930, 108.
doi:10.3847/1538-4357/ac6588
- Wang, J.-M. & Bon, E. 2020, *A&A*, 643, L9.
doi:10.1051/0004-6361/202039368
- Wang, W., Bu, D.-F., & Yuan, F. 2022, *Monthly Notices of the Royal Astronomical Society*, 513, 5818.
doi:10.1093/mnras/stac1348

Yang, X.-H., Ablimit, K., & Li, Q.-X. 2021, The
Astrophysical Journal, 914, 31.
doi:10.3847/1538-4357/abf8b5

Yang, J., Paragi, Z., Beswick, R. J., et al. 2021, MNRAS,
503, 3886. doi:10.1093/mnras/stab706
Yang, Q., Wu, X.-B., Fan, X., et al. 2018, ApJ, 862, 109.
doi:10.3847/1538-4357/aaca3a